https://doi.org/10.5194/essd-2019-70
Preprint. Discussion started: 18 July 2019


Open Access Earth System Science Data Discussions

# A Maximum Entropy Production Evaporation - Transpiration Product for Australia

Olanrewaju Abiodun[1], Okke Batelaan[1] Huade Guan[1], and Jingfeng Wang[2]

1. National Centre for Groundwater Research and Training, College of Science and Engineering, Flinders University, Australia
2. School of Civil and Environmental Engineering, Georgia Institute of Technology, Atlanta, USA

Corresponding author:

Olanrewaju Abiodun, College of Science and Engineering, Flinders University, Bedford Park, Australia, lanre.abiodun@flinders.edu.au

**Abstract**

The aim of this research is to develop evaporation and transpiration products for Australia based on the maximum entropy production model (MEP). We introduce a method into the MEP algorithm of estimating the required model parameters over the entire Australia through the use of pedotransfer function, soil properties and remotely sensed soil moisture data. Our algorithm calculates the evaporation and transpiration over Australia on daily timescales at the 5 km$^2$ resolution for 2003 – 2013.

The MEP evapotranspiration (ET) estimates are validated using observed ET data from 20 Eddy Covariance (EC) flux towers across 8 land cover types in Australia. We also compare the MEP ET at the EC flux towers with two other ET products over Australia; MOD16 and AWRA-L products. The MEP model outperforms the MOD16 and AWRA-L across the 20 EC flux sites, with average root mean square errors (RMSE), 8.21, 9.87 and 9.22 mm/8 days respectively. The average mean absolute error (MAE) for the MEP, MOD16 and AWRA-L are 6.21, 7.29 and 6.52 mm/8 days, the average correlations are 0.64, 0.57 and 0.61, respectively. The percentage Bias of the MEP ET was within 20% of the observed ET at 12 of the 20 EC flux sites while the MOD16 and AWRA-L ET were within 20% of the observed ET at 4 and 10 sites respectively. Our analysis shows that evaporation and transpiration contribute 38% and 62%, respectively, to the total ET across the study period which includes a significant part of the "millennium drought" period (2003 – 2009) in Australia. The data (Abiodun et al., 2019) is available at http://dx.doi.org/10.25901/5ce795d313db8

https://doi.org/10.5194/essd-2019-70
Preprint. Discussion started: 18 July 2019


Open Access Earth System Science Data Discussions

.

*Keywords:* Evaporation; transpiration; Maximum Entropy Production; remote sensing

## 1. Introduction

The use of remote sensing data in existing and new methods for evapotranspiration (ET) estimation is incontrovertibly the current and future trend of ET flux quantification on catchment, regional and continental scales (Bhattarai et al., 2016;Zhang et al., 2016;Najmaddin et al., 2017). The use of remote sensing observations is an unprecedented advancement in regional scale ET estimation due to its spatiotemporal flexibility and/or economic viability (Chirouze et al., 2014;Long et al., 2014;Xiong et al., 2014;Yang et al., 2015;Bhattarai et al., 2016). Various methods have been developed for improving ET estimates (Allen et al., 2007;Cleugh et al., 2007;Tang et al., 2009;Mu et al., 2011;Xiong et al., 2014). However, the relative accuracy of these methods differ across different climates, vegetation and soil types (Jia et al., 2012;Kim et al., 2012;Velpuri et al., 2013;Bhattarai et al., 2016). The performance of the ET models depends on the parameterization of physical processes underlying ET (Liaqat and Choi, 2017). A major challenge is to produce accurate ET estimates of various spatial and temporal resolutions (Senay et al., 2013;Wang et al., 2016;Gaur et al., 2017) when using remote sensing data (Kalma et al. (2008).

A remote sensing based ET model is empirical or physically-based (Xiong et al., 2014). In the past two decades, several physically based ET models have been developed including the single source energy balance (SSEB) (Bastiaanssen et al., 1998;Roerink et al., 2000;Allen et al., 2007) and two-source surface energy balance (TSEB) (Kustas and Norman, 1999;Norman et al., 2003;Sun et al., 2009) models using remote sensing input data. The SSEB models provide total ET without partitioning it into soil evaporation (E) and transpiration (T), while the TSEB models do the partition. The TSEB models have been shown to be more accurate over partially vegetated surfaces (Timmermans et al., 2007;Gao and Long, 2008;Choi et al., 2009). A fundamental challenge of TSEB models is their reliance on land surface temperature (LST) and the partitioning methodology of the LST into soil and canopy temperature components for modelling (Colaizzi et al., 2012;Yang et al., 2018). Different techniques have been applied to partition the canopy and soil temperatures from the LST in the TSEB models (Norman et al., 2000;Zhang et al., 2005), with varying degree of success over different vegetation types (Chavez et al., 2009;Song et al., 2016;Diarra et al., 2017). The more pertinent challenge of the TSEB models becomes apparent when creating high resolution regional to continental scale ET, which requires accurate LST data as the

https://doi.org/10.5194/essd-2019-70
Preprint. Discussion started: 18 July 2019


principal input. Frequent clouds plague remotely sensed LST products such as the widely accepted Moderate Resolution Imaging Spectroradiometer land surface temperature product (MODIS LST) (Wan et al., 2002).

The limitations of the LST dependence of the traditional TSEB models was further highlighted by Mu et al. (2007) who found that the use of the 8-day composite of all cloud free data in the MODIS LST suite did not produce accurate estimates of global scale evapotranspiration. The MODIS LST yielded erroneous results of partitioned soil and canopy temperatures across various biomes, hence the development of a new algorithm is needed for estimating soil and canopy temperatures for improving the MODIS ET product (MOD16), which is widely accepted for comparison and validation purposes on catchment to continental scales. There are, however, unresolved issues of accuracy (Tang et al., 2015;de Arruda Souza et al., 2018;Khan et al., 2018). With the challenge surrounding the LST partitioning in TSEB models and the MOD16 challenges, a different perspective to the TSEB modelling on regional scale is required.

The Maximum Entropy Production (MEP) model of ET (Wang and Bras, 2011) is a new approach to modelling ET. The MEP model was formulated as a unique TSEB model for soil and vegetated surface where ET and the other surface heat fluxes result from the partition of net radiation. The MEP model requires three main inputs: surface temperature, specific humidity and net radiation. A major departure of the MEP model from the traditional TSEB models is that the MEP model is less sensitive to temperature and more sensitive to the moisture content of immediately above the target surface and the available energy.

Case studies have shown that the MEP ET for small catchments outperformed several other models (Nearing et al., 2012;Yang and Wang, 2014;Shanafield et al., 2015). However, the MEP ET model is yet to be comprehensively tested over various vegetation covers. A global product of the MEP ET at a 100 km$^2$ spatial resolution has been produced (Huang et al., 2017). However, at this scale, individual vegetation cover type validation and analysis is problematic. The ET data over the diverse Australian landscape at catchment to continental scale has been produced (Guerschman et al. (2009) using MOD16 model (Mu et al., 2011) and the Australian Water Resource Assessment Landscape (AWRA-L) model (Viney et al., 2014).

The goal of this paper is to develop a daily MEP ET product for Australia on a 0.05$^{o}$ spatial resolution. We have generated the data for 2003 – 2013 for demonstration and testing of result (Abiodun et al., 2019). The skill of the MEP ET model will be evaluated using eddy covariance tower data across various vegetation covers and

https://doi.org/10.5194/essd-2019-70
Preprint. Discussion started: 18 July 2019


compared with the results of the MOD16 and the AWRA-L products. The evaluation period covers the climatological highly variable "millennium drought" period (2003-2010).

## 2 Method and data

The energy balance equation over the land surface is expressed as,

$$E + H + G = R_n \tag{1}$$

where $E, H, G$ and $R_n$ are evapotranspiration (W/m$^2$), sensible heat (W/m$^2$), ground heat (W/m$^2$) and net radiation (W/m$^2$), respectively. The MEP ET model provides a solution of $Es, Hs,$ and $G$ over non-vegetated land surface satisfying the energy balance equation Eq. (1) (Wang and Bras (2011) for given net radiation Rn, surface temperature T, and surface specific humidity q,

$$\sigma_s = \frac{\lambda^2}{c_p R_v}\frac{q_s}{T_s^2}\ ,\ \ \beta(\sigma_s) = 6\left(\sqrt{1+\frac{11}{36}\sigma_s - 1}\right) \tag{2}$$

$$G = \frac{\beta(\sigma_s)}{\sigma_s}\frac{I_s}{I_o}\,H_s|H_s|^{-\frac{1}{6}} \tag{3}$$

$$E_s = \beta(\sigma_s)H_s \tag{4}$$

where $\sigma_s$ (Sigma) is a dimensionless parameter characterizing the effect of (soil or canopy) surface thermal and moisture state on the phase change of liquid water (-); $\lambda$ is the latent heat of vaporization of liquid water (J kg$^{-1}$); $c_p$ is the specific heat of dry air at constant pressure (J kg$^{-1}$ K$^{-1}$); $R_v$ is the gas constant of water vapor (J kg$^{-1}$ K$^{-1}$); $q_s$ the specific humidity at the soil or vegetation surface (kg kg$^{-1}$); $T_s$ is the soil or canopy surface temperatures (K); $\beta(\sigma_s)$ is the inverse Bowen ratio (-); $I_s$ is the thermal inertia of soil (J m$^{-2}$ K$^{-1}$ s$^{-1/2}$); $I_o$ is the thermal inertia of turbulent air (J m$^{-2}$ K$^{-1}$ s$^{-1/2}$). For vegetated land surface where $G$ is neglected, equations (2) – (4) become;

$$E_v = \frac{R_{n\_v}}{1+\sigma_s{}^{-1}}\ , H_v = \frac{R_{n\_v}}{1+\sigma_s} \tag{6}$$

https://doi.org/10.5194/essd-2019-70
Preprint. Discussion started: 18 July 2019



where $E_v$ is the canopy transpiration and $H_v$ sensible heat flux over canopy surface satisfying energy balance equation $R_n = E_v + H_v$.

The MEP ET algorithm calculates soil evaporation and canopy transpiration separately. Total evapotranspiration is the sum of the two fluxes weighted by the fractional coverage of soil and canopy (Fig 1). In this paper, we apply temporally varying vegetation fraction cover in the algorithm to partition the radiation energy for soil and canopy.

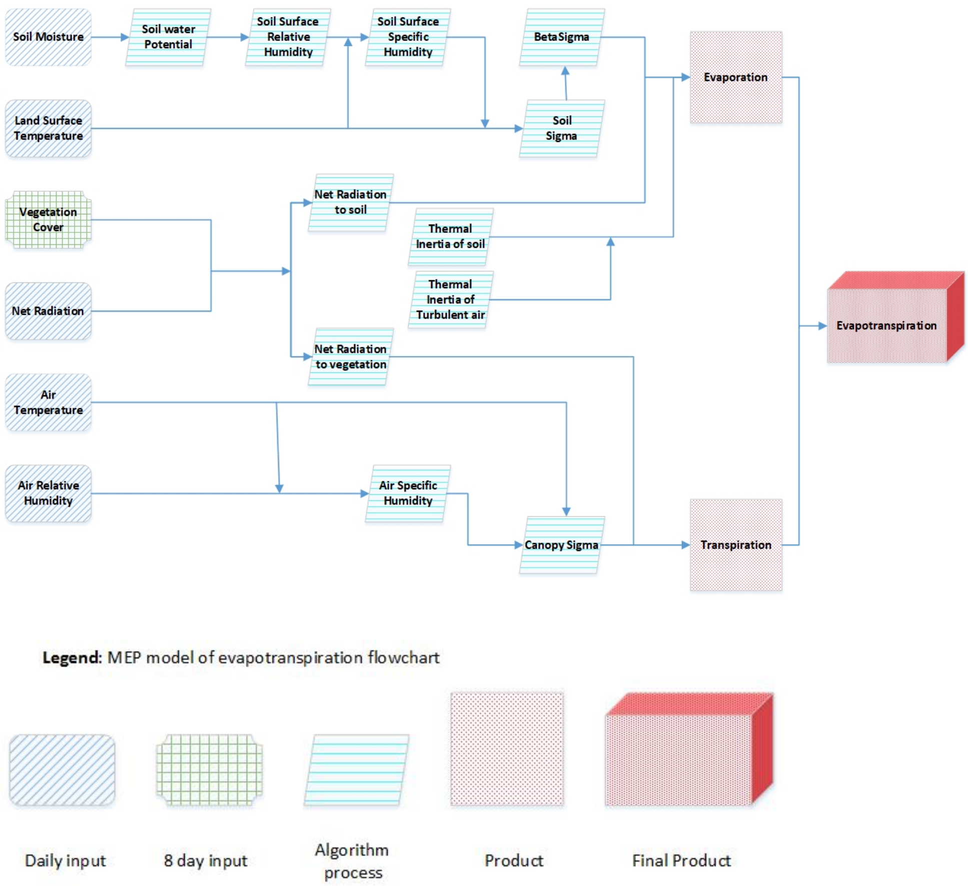


*Figure 1: Flowchart of MEP ET algorithm; BetaSigma is the inverse Bowen ratio*

## 2.1 Net radiation ($R_n$)

https://doi.org/10.5194/essd-2019-70
Preprint. Discussion started: 18 July 2019




Daily net radiation at 0.05° spatial resolution over Australia is partitioned between soil and canopy within a grid cell according to vegetation fraction cover. Photosynthetically active radiation (FPAR) product MOD15A2H (Myneni et al., 2015) is used in this study. While the MEP model is very sensitive to net radiation as a model input with pronounced diurnal cycle, 8-day vegetation cover data were used as vegetation cover changes at seasonal time scale. Net radiation over canopy and soil surface within a grid cell is expressed as,

$$R_{n\_v} = F_c\, R_n \ ,\ R_{n\_s} = (1 - F_c)\, R_n \tag{7}$$

where, $R_{n\_v}$ is the net radiation over vegetation (W/m$^2$), $R_{n\_s}$ is the net radiation over soil (W/m$^2$), and $F_c$ is the vegetation fraction (-).

## 2.2 Evaporation

The MEP model as in Eqs. 1, 3 and 4 provides a unique solution of E, G and H for given surface temperature ($T_s$), soil/canopy surface specific humidity ($q_s$), and $R_{n\_s}$. The land surface temperature ($T_s$) is provided by the MOD11C1 product (Wan, 2014) derived from the MODIS observations. The daily data for Australia from 2003 to 2013 was extracted from the global dataset. Missing $T_s$ data, due to cloud cover, were filled using the lowest value within a month for each grid cell. The rationale is that cloud cover reduces the amount of solar radiation reaching the land surface, hence the lowest observed $T_s$ value within a month is used.

Due to the difficulty of obtaining $q_s$ over the entire Australia, an empirical equation is used to calculate $q_s$ as a function of soil surface relative humidity and land surface temperature. The soil surface relative humidity is calculated from the soil surface water potential. The Hutson and Cass function (Hutson and Cass (1987) is used for estimating soil surface water potential. The Hutson & Cass function requires two empirical coefficients calibrated for each grid cell using two methods: the empirical equation derived in Williams et al. (1992), and the pedotransfer functions to estimate the soil water content at wilting point (-1.5MPa) and at field capacity (-10kPa). The water content at the wilting point and field capacity for each 0.05° grid cell, estimated from the pedotransfer functions, are subsequently used to determine the coefficients, by applying the two-point method (Cresswell and Paydar (1996) (see Section 2.3.1). Different pedotransfer functions for determining the wilting point and field capacity (Minasny et al., 1999;Minasny and Mcbratney, 2002;Rab et al., 2011) (see Equations. 12 and 13 in (Rab et al. (2011)) were selected due to their modest data requirement and relative accuracy. The pedotransfer function combined with the two point method was preferred to the empirical equations (Williams et al. (1992) as they

https://doi.org/10.5194/essd-2019-70
Preprint. Discussion started: 18 July 2019


yielded significantly better estimates of ET after validation with flux tower data. Soil properties as the inputs of the pedotransfer functions and empirical equations are obtained from the Australian Soil Resource Information System (ASRIS) (Johnston et al., 2003).

An important parameter of the MEP model is the distance above target surface for which the Monin-Obukhov similarity theory is valid ($z$) in the formula of the thermal inertia of turbulent air above soil surface. Huang et al. (2017) suggested that the distance above target ($z$) vary with the land cover types as shown in the look-up table (Table 1) used in this study. $z$ for each land cover is specified for each 0.05° grid cell using the MODIS land cover product (MOD12C1) (Mark and Damien, 2015) of the same resolution.

*Table 1: Distance above target surface (z) in (m) for Australian Land cover*

| Land Cover | Distance above target (z) in (m) |
|---|---|
| Evergreen Needleleaf Forests (ENF) | 10 |
| Evergreen Broadleaf Forests (EBF) | 10 |
| Deciduous Needleleaf Forests (DNF) | 10 |
| Deciduous Broadleaf Forests (DBF) | 10 |
| Mixed Forests (MF) | 10 |
| Closed Shrublands (CSH) | 5 |
| Open Shrublands (OSH) | 4 |
| Woody Savannas (WSA) | 8 |
| Savannas (SAV) | 7 |
| Grasslands (GRA) | 5 |
| Croplands (CRP) | 5 |
| Urban and Built up (URB) | 3 |
| Cropland/Natural Vegetation Mosaics (CRV) | 5 |

https://doi.org/10.5194/essd-2019-70
Preprint. Discussion started: 18 July 2019


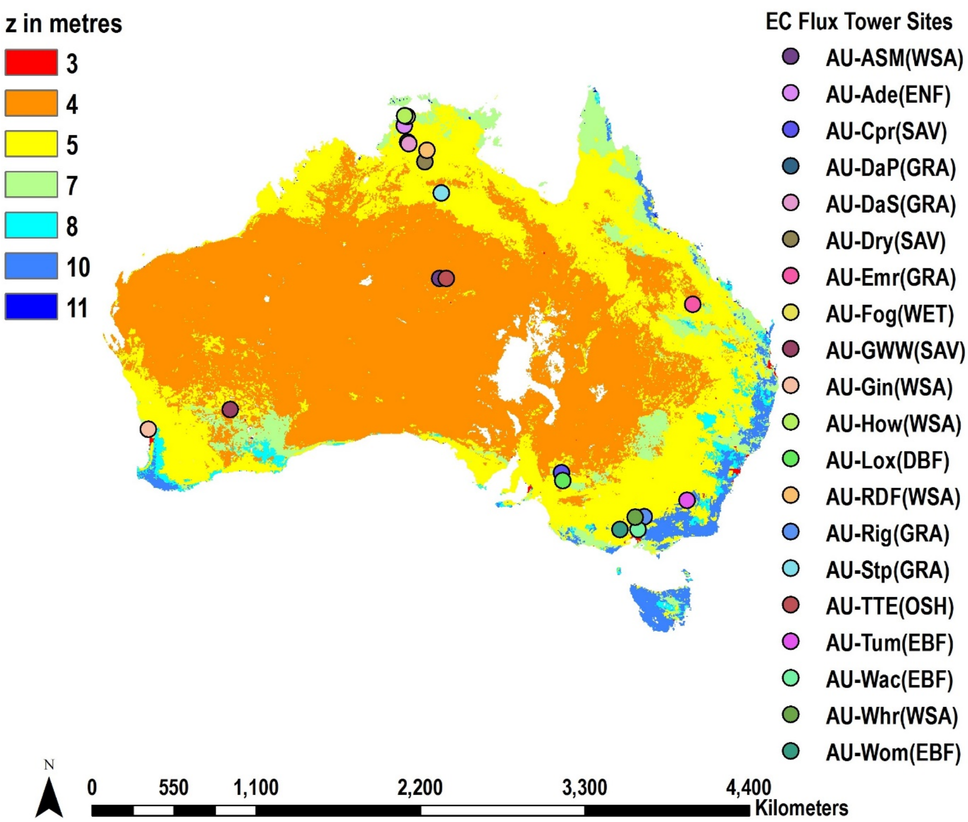


*Figure 2: Target height (z) in (m) above vegetation with location of Eddy Covariance flux towers and the land cover types;*

**2.2.1 Hutson and Cass function with the two-point method**

To determine the Hutson and Cass coefficients “a” and “b” (Eq. 14) for each 0.05° grid cell across Australia, we solve the pedotransfer with the two-point method. The two values used are the volumetric soil moisture (θ1 and θ2) at the field capacity and the wilting point soil water potentials (Ψ1 and Ψ2) of -10 kPa and 1500 kPa respectively. Combining both equations, we obtain the model parameters “a” and “b” for each 0.05° grid cell.

$$\Psi = a\left(\frac{\theta}{\theta_p}\right)^{-b} \tag{8}$$

$$\theta_p = 1 - (\rho / \rho_s) \tag{9}$$

where Ψ is the soil water potential (kPa); a (kPa) and b (-) are curve-fitting parameters; $\theta_p$ (-) is the porosity; ρ ($kg/dm^3$) is the bulk density of soil; and $\rho_s$ =2.65 ($kg/dm^3$) is the mineral density.

https://doi.org/10.5194/essd-2019-70
Preprint. Discussion started: 18 July 2019


Open Access Earth System Science Data Discussions

### 2.2.2 Soil moisture

The soil moisture data used in this study are obtained from the European Space Agency's Climate Change Initiative Soil Moisture Project (ESA CCI SM) at 0.25° and daily resolution available from 1978 to 2018 (Dorigo et al., 2017), hereafter referred to as the ESA CCI SM. The ESA CCI SM consists of three products; Active, Passive and Combined (Liu et al., 2012;Gruber et al., 2017). The ESA CCI SM is preferred in this study as it offers the most suitable spatio-temporal resolution compared to other available soil moisture products. The combined product is selected in this study as its algorithm unifies the Active and Passive products to have better spatial coverage than either the Passive or Active products with more stringent quality control. While the combined product has good spatial-temporal resolution for remote sensing applications, missing data are filled through an average of the day before and after. Multiple-days data gaps are filled using multiple-days average. The ESA CCI SM is also resampled at 0.05° resolution to be consistent with the spatial resolutions of the other input data.

## 2.3 Transpiration

The MEP method requires specific humidity and temperature very close to the target surface. However due to the difficulty of obtaining leaf surface temperature and specific humidity at regional scales, air temperature and air specific humidity are used as surrogates. Air temperature and relative humidity data above canopy are obtained from the interpolated field observations over Australia (Jeffrey et al., 2001). The Clausius-Clapeyron equation is used in obtaining the specific humidity from air temperature and relative humidity.

## 2.4 Model Evaluation

For the evaluation of the MEP model results over Australia, data from 20 eddy covariance (EC) flux towers across different land covers are used. The model performance is evaluated using six statistical metrics: the root mean square error ($RMSE$), mean difference ($MD$), mean absolute error ($MAE$), Pearson's correlation coefficient (R), Nash-Sutcliffe Efficiency ($NSE$) and Percent Bias ($PBIAS$),

$$RMSE = \sqrt{\frac{\sum_{n=1}^{N}(Q_n - \widehat{Q_n})^2}{N}} \tag{10}$$

$$MD = \frac{\sum_{n=1}^{N}(Q_n - \widehat{Q_n})}{N} \tag{11}$$

$$MAE = \frac{\sum_{n=1}^{N}|Q_n - \widehat{Q_n}|}{N} \tag{12}$$

$$R = \frac{(\sum_{n=1}^{N}(Q_n - \overline{Q})(\widehat{Q_n} - \widetilde{Q_n}\ )}{\sqrt{\sum_{n=1}^{N}(Q_n - \overline{Q})^2}\sqrt{\sum_{n=1}^{N}(\widehat{Q_n} - \widetilde{Q_n})^2}} \tag{13}$$

$$NSE\ = 1 - \frac{\sum_{n=1}^{N}(Q_n - \widehat{Q_n})^2}{\sum_{n=1}^{N}(Q_n - \overline{Q})^2} \tag{14}$$

https://doi.org/10.5194/essd-2019-70
Preprint. Discussion started: 18 July 2019


$$PBIAS = 100 \times \frac{\sum_{n=1}^{N}(Q_n - \widehat{Q_n})}{\sum_{n=1}^{N} Q_n} \tag{15}$$

where $x_n$ and $y_n$ are observed and simulated daily ET values (mm); $N$ is the number of observed or simulated ET values; $Q_n$ (mm) is the measured ET at day $n$; $\widehat{Q_n}$ (mm) is the simulated ET at day $n$; $\widetilde{Q_n}$ (mm) is the mean simulated discharge at day $n$; and $\overline{Q}$ (mm) is the mean ET.

The MEP ET product at 5 km$^2$ resolution is validated across the 20 EC tower flux data with footprints ranging from 100 m$^2$ up to about 2 km$^2$ depending on the measuring height of the EC system and vegetation height. The effects of the differences in footprints of the EC towers and the data to be validated are not considered in this study.

A three-product comparison (MEP, AWRA-L and MOD16) with the field data from the 20 EC flux towers across Australia was conducted as part of this study. While the MEP and the AWRA-L models are produced on daily timescales, the MOD16's highest temporary resolution is an 8-day product. For a direct comparison, MEP and AWRA-L are aggregated to 8-day resolution. Since the MOD16 dataset has missing data points due to cloud cover or sensor failures, the days with missing data are removed across all models and the EC tower data before comparison.

Mean annual maps are produced for the three products between 2003 and 2013 with the MOD16 resampled to the 5 km$^2$ resolution to match that of the MEP and AWRA-L data for direct comparison for 280,000 pixels covering the entire Australian using the R, RMSE, MAE and NSE statistical metrics.

## 3. Results and discussion

### 3.1 Mean spatial-temporal MEP ET Analysis

The daily MEP evaporation and transpiration over Australia for 2003 – 2013 are relatively high in the northern vegetated parts of Australia (Fig. 3a-b) and around the eastern coastline (Fig. 3b). Evaporation and transpiration account for 38% and 62% of total ET, respectively, over Australia. ET is highest in the high rainfall shrub-lands and forested regions in the northern Australia as well as around the coastline (Fig 3c). The west central parts of Australia have the lowest ET with mean annual ET 440 mm for Australia for 2003-2013, while the mean ET along the coastline exceeds 1000 mm for the same period.

https://doi.org/10.5194/essd-2019-70
Preprint. Discussion started: 18 July 2019


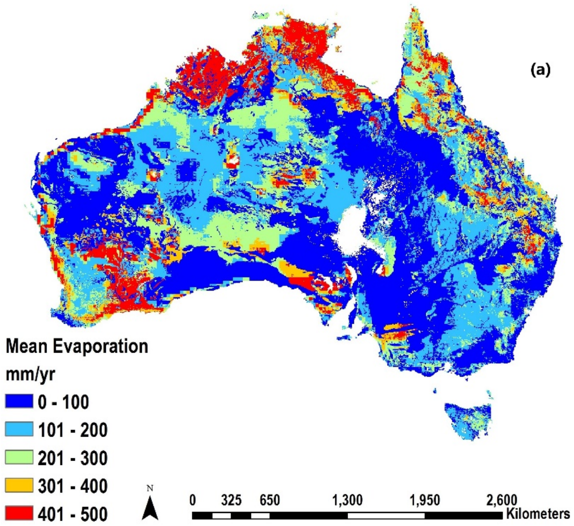


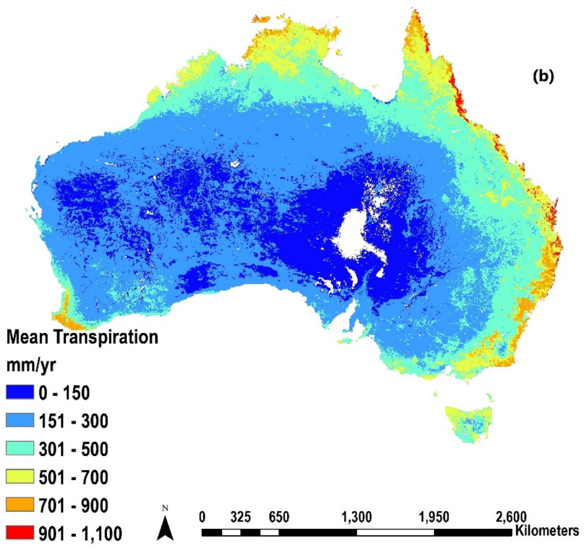

https://doi.org/10.5194/essd-2019-70
Preprint. Discussion started: 18 July 2019


Open Access Earth System Science Data Discussions

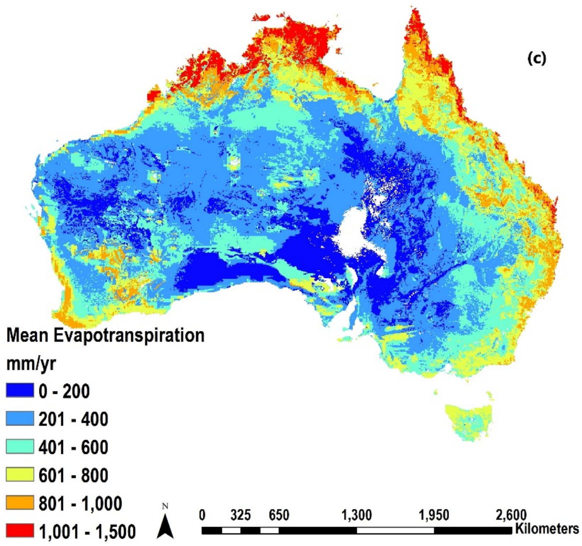


*Figure 3: (a) Mean evaporation; (b) Mean transpiration; and (c) Mean evapotranspiration in mm/yr for 2003-2013*

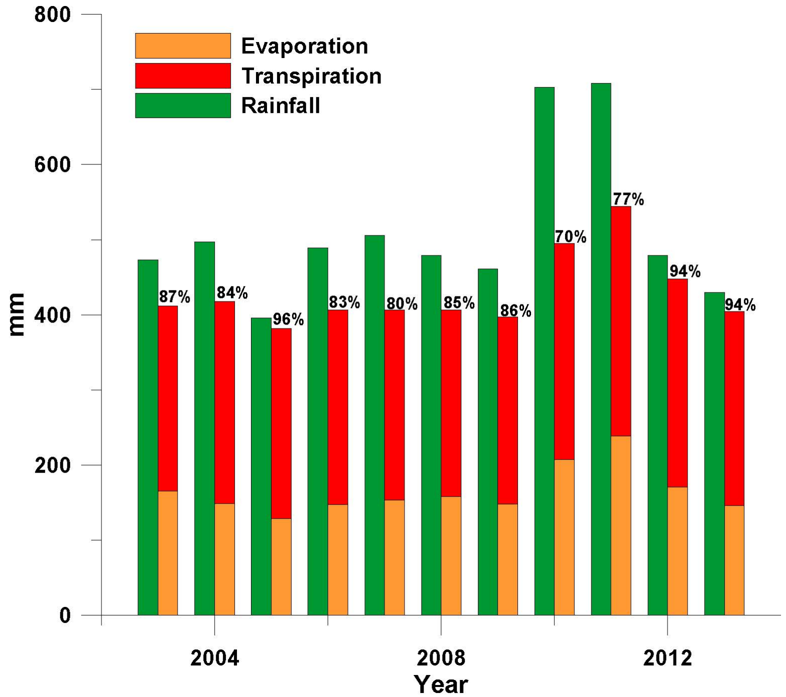


*Figure 3: MEP E &T vs Rainfall*

https://doi.org/10.5194/essd-2019-70
Preprint. Discussion started: 18 July 2019


Annual ET fluctuates during the study period (Fig 3) with the correlations between annual evaporation and transpiration and annual rainfall 0.94 and 0.84, respectively. Although the MEP model does not use rainfall as an input, the strong correlation between rainfall and ET, the largest components of the hydrologic system in Australia, suggests the MEP model captures the Australian hydrological system effectively. These results are consistent with the findings of Jung et al. (2010) who observed a drop in the global evapotranspiration due to reduced ET over Australia between 1998 and 2008. The reduction in ET over Australia can be seen through the "millennium drought" years with the immediate increase in ET observed in 2010 at the end of the prolonged drought.

https://doi.org/10.5194/essd-2019-70
Preprint. Discussion started: 18 July 2019


Open Access Earth System Science Data Discussions

*Table 2: EC validation of the MEP, MOD16 and AWRA-L products. Eddy Covariance Tower Site name (Site Name); Fluxnet site ID and IGBP land cover type (Site ID); Average observed ET at flux tower (OBS_ET); Root Mean Square Error (RMSE); Mean Absolute Error (MAE); Correlation Coefficient (R); Percent Bias (PBIAS); EC sites citations*

| **Site Name** | **Site ID** | **Obs_ET (mm/ 8 days)** | **RMSE (mm/ 8 days)** | | | **MAE (mm/ 8 days)** | | | **R** | | | **PBIAS (%)** | | | **Citations** |
|---|---|---|---|---|---|---|---|---|---|---|---|---|---|---|---|
| | | | MEP | MOD16 | AWRA-L | MEP | MOD16 | AWRA-L | MEP | MOD16 | AWRA-L | MEP | MOD16 | AWRA-L | |
| Adelaide River | AU-Ade (WSA) | 15.34 | **9.06** | 11.09 | 9.65 | 7.04 | 9.22 | **5.73** | 0.64 | 0.57 | **0.71** | 26.18 | -34.38 | **22.26** | (Beringer, 2014g) |
| Alice Springs | AU-ASM (ENF) | 8.45 | **6.12** | 8.82 | 7.13 | **4.80** | 6.05 | 6.03 | **0.74** | 0.69 | 0.63 | **-6.78** | -62.1 | -23.9 | (Derek and James, 2014a) |
| Calperum | AU-Cpr (SAV) | 8.39 | **3.38** | 4.69 | 3.55 | **1.01** | 2.79 | 1.27 | 0.62 | 0.33 | **0.72** | **-12.04** | -33.25 | -15.15 | (Koerber, 2014) |
| Daly River Cleared | AU-DaS (GRA) | 18.6 | **4.62** | 9.74 | 6.05 | **3.63** | 8.21 | 4.43 | **0.88** | 0.74 | 0.78 | -12.23 | -38.6 | **0.21** | (Beringer, 2014f) |
| Daly River Savanna | AU-DaP (GRA) | 12.24 | 10.43 | 10.75 | **9.78** | 8.64 | 6.93 | **6.89** | 0.63 | 0.74 | **0.77** | 17.32 | **13.86** | 41.49 | (Beringer, 2014f) |
| Dry River | AU-Dry (SAV) | 19.55 | **9.95** | 13.63 | 12.58 | **4.7** | 8.14 | 5.02 | **0.62** | 0.43 | 0.58 | **-24.2** | -41.77 | -25.8 | (Beringer, 2014e) |
| Emerald | AU-Emr (GRA) | 11.56 | **5.69** | 5.96 | 9.91 | **4.22** | 4.35 | 7.32 | 0.47 | **0.48** | 0.43 | **-10.92** | -14.38 | 21.25 | (Schroder, 2014) |
| Fogg Dam | AU-Fog (WET) | 35.35 | **15.45** | 22.53 | 18.9 | **13.97** | 20.72 | 16.33 | 0.26 | 0.6 | **0.61** | **-35.71** | -58.4 | -42.79 | (Beringer, 2013b) |
| Gingin | AU-Gin (WSA) | 15.47 | 6.27 | 7.21 | **5.49** | 5.20 | 6.09 | **4.1** | 0.39 | 0.37 | **0.51** | **-3.0** | -36.49 | -17.02 | (Silberstein, 2015) |
| Great Western Woodlands, | AU-GWW (SAV) | 7.65 | **2.78** | 5.15 | 3.47 | **2.04** | 3.9 | 2.62 | **0.63** | 0.08 | 0.37 | 11.08 | -47.45 | **-11.06** | (Craig, 2014;Beringer, 2014d) |
| Howard Springs | AU-How (WSA) | 24.96 | **7.13** | 9.92 | 7.96 | **5.53** | 8.13 | 6.18 | 0.67 | 0.79 | 0.79 | **-3.2** | -30.0 | -9.87 | (Beringer, 2014c) |
| Loxton | AU-Lox (DBF) | 27.3 | 27.31 | **27.09** | 32.63 | 17.78 | **17.51** | 22.8 | **0.51** | 0.37 | -0.12 | -63.48 | **-60.0** | -82.7 | (Ewenz, 2008) |
| Red Dirt Melon Farm | AU-RDF (WSA) | 14.66 | **9.56** | 11.36 | 12.17 | **8.25** | 8.65 | 8.88 | **0.66** | 0.55 | 0.58 | **3.45** | -25.39 | 12.53 | (Beringer, 2013a) |
| Riggs Creek | AU-Rig (GRA) | 13.22 | 5.72 | 9.07 | **4.53** | 4.67 | 4.23 | **3.28** | 0.71 | 0.70 | **0.83** | -14.96 | -22.21 | **11.62** | (Beringer, 2014b) |
| Sturt Plains | AU-Stp (GRA) | 10.24 | **7.95** | 8.20 | 8.5 | 6.17 | 5.64 | **4.79** | 0.73 | **0.79** | 0.78 | 25.77 | -40.4 | **17.9** | (Schroder, 2014) |

https://doi.org/10.5194/essd-2019-70
Preprint. Discussion started: 18 July 2019


| | | | | | | | | | | | | | | | |
|---|---|---|---|---|---|---|---|---|---|---|---|---|---|---|---|
| Ti Tree East | AU-TTE (OSH) | 2.81 | 4.45 | **4.32** | 6.99 | 3.69 | **2.63** | 4.95 | **0.43** | 0.08 | 0.20 | 96.17 | **-42.34** | 146.08 | (Derek and James, 2014b) |
| Tumbarumba | AU-Tum (EBF) | 20.86 | 6.72 | 6.54 | **5.97** | 4.75 | 4.98 | **4.31** | 0.83 | 0.86 | 0.86 | -13.82 | 14.07 | **-6.57** | (Woodgate, 2014) |
| Wallaby Creek | AU-Wac (EBF) | 15.35 | 6.76 | 11.13 | **5.76** | 5.82 | 9.31 | **4.84** | **0.85** | 0.77 | 0.78 | 34.67 | 57.75 | **25.57** | (Beringer, 2014a) |
| Whroo | AU-Whr (WSA) | 13.73 | 6.51 | **5.08** | 5.86 | 5.09 | **4.10** | 4.52 | 0.54 | **0.59** | 0.46 | **-2.54** | -23.07 | -10.8 | (Beringer, 2014d) |
| Wombat | AU-Wom (EBF) | 23.28 | 8.24 | **5.13** | 7.45 | 7.11 | **4.16** | 6.02 | **0.89** | 0.88 | 0.81 | -30.12 | **-0.29** | -21.24 | (Beringer, 2014h) |

https://doi.org/10.5194/essd-2019-70
Preprint. Discussion started: 18 July 2019


### 3.2 MEP, MOD16 and AWRA-L performances at the Eddy Covariance flux sites

The 20 eddy covariance flux tower sites used for the validation of the MEP, MOD16 and AWRA-L products include 8 land cover types according to the International Geosphere-Biosphere Programme (IGBP), i.e. 4-Evergreen Broadleaved Forest (EBF), 4-Woodland Savanna (WSA),4-Savanna (SAV), 1-Wetland (WET), 4-Grassland (GRA), 1-Evergreen Needle Forest (ENF), 1-Deciduous Broadleaved Forest (DBF), and 1-Open Shrubland (OSH). The MEP model outperforms the MOD16 at 15, 13, 14 and 16 sites measured by the RMSE, MAE, R and PBIAS metrics respectively. The MEP also performed better than the AWRA-L at 13, 11, 11 and 12 sites measured by the RMSE, MAE, R and PBIAS metrics, respectively. The MEP model also outperforms the MOD16 and AWRA-L measured by the average RMSE, MAE and R across the 20 EC flux sites. The average RMSE across the 20 EC flux sites for the MEP, MOD16 and AWRA-L are respectively 8.21, 9.87 and 9.22. The average MAE are respectively 6.21, 7.29 and 6.52 for the MEP, MOD16 and AWRA-L. The average correlations are 0.64, 0.57 and 0.61 for the MEP, MOD16 and AWRA-L, respectively. The MEP PBIAS was within 20% of the observed flux at 12 sites while the MOD16 and AWRA-L were within 20% of the observed flux at 4 and 10 sites, respectively.

Some consistency is seen across the models at many sites, with the three models seeming to perform best for the evergreen broadleaved forests with correlations ranging from 0.77 to 0.89 at the three sites. Similar correlation consistency of the models is obtained across the five grassland sites. Generally, the MOD16 underestimated ET significantly at most sites with 12 sites over 30%. Consistent underestimation is also observed across the Fogg Dam wetland site with the three models underestimating ET by 35% or higher. The MEP ET exhibited the lowest correlation at the Fogg Dam site. The Fogg Dam is a seasonally flooded wetland where water evaporation is a principal component of ET. However, due to the coarse resolution of the soil moisture data, the MEP model may not effectively capture the local evaporation. Less accurate ET estimates were also observed at the Loxton site by the three models with underestimation at least 60%. The flux data at the Loxton site appear unrealistic presumably caused by sensor failures suggested by 1800 mm ET while only 500 mm rainfall is recorded at the site.

https://doi.org/10.5194/essd-2019-70
Preprint. Discussion started: 18 July 2019


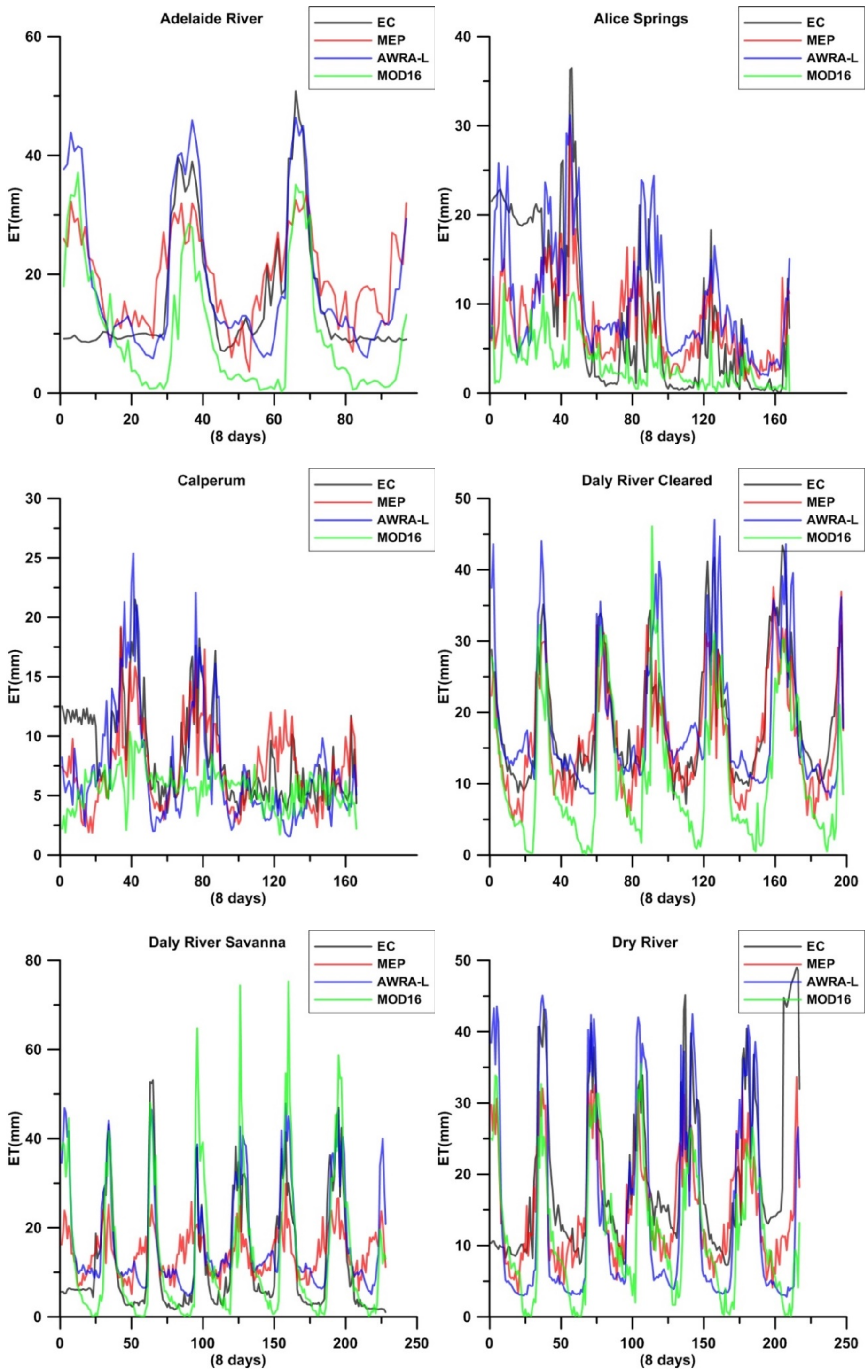

https://doi.org/10.5194/essd-2019-70
Preprint. Discussion started: 18 July 2019


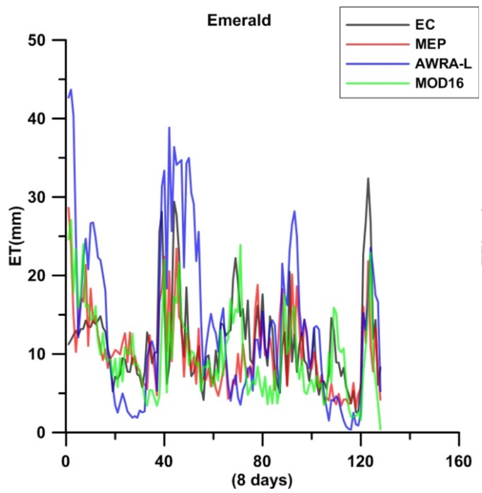


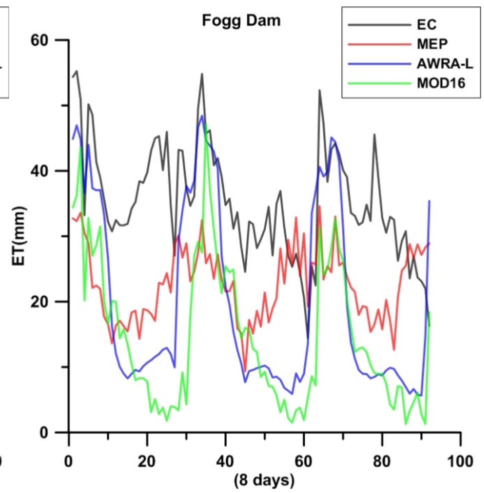


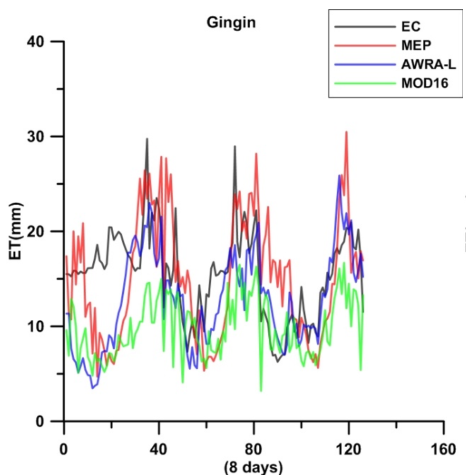


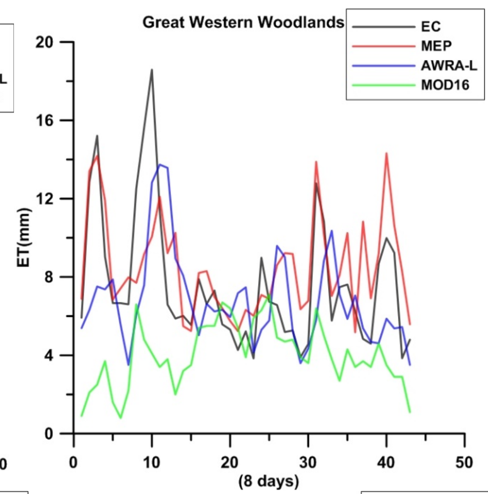


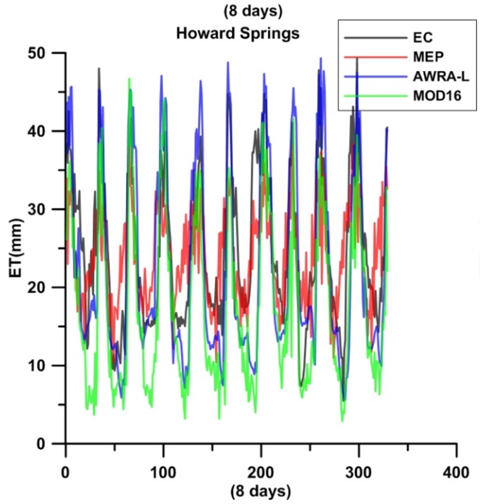


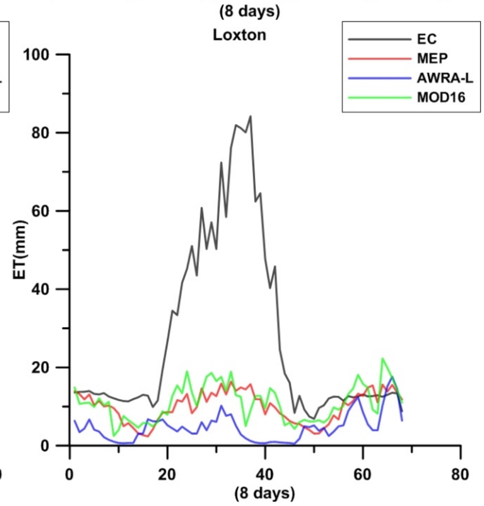

https://doi.org/10.5194/essd-2019-70
Preprint. Discussion started: 18 July 2019


Open Access Earth System Science Data Discussions

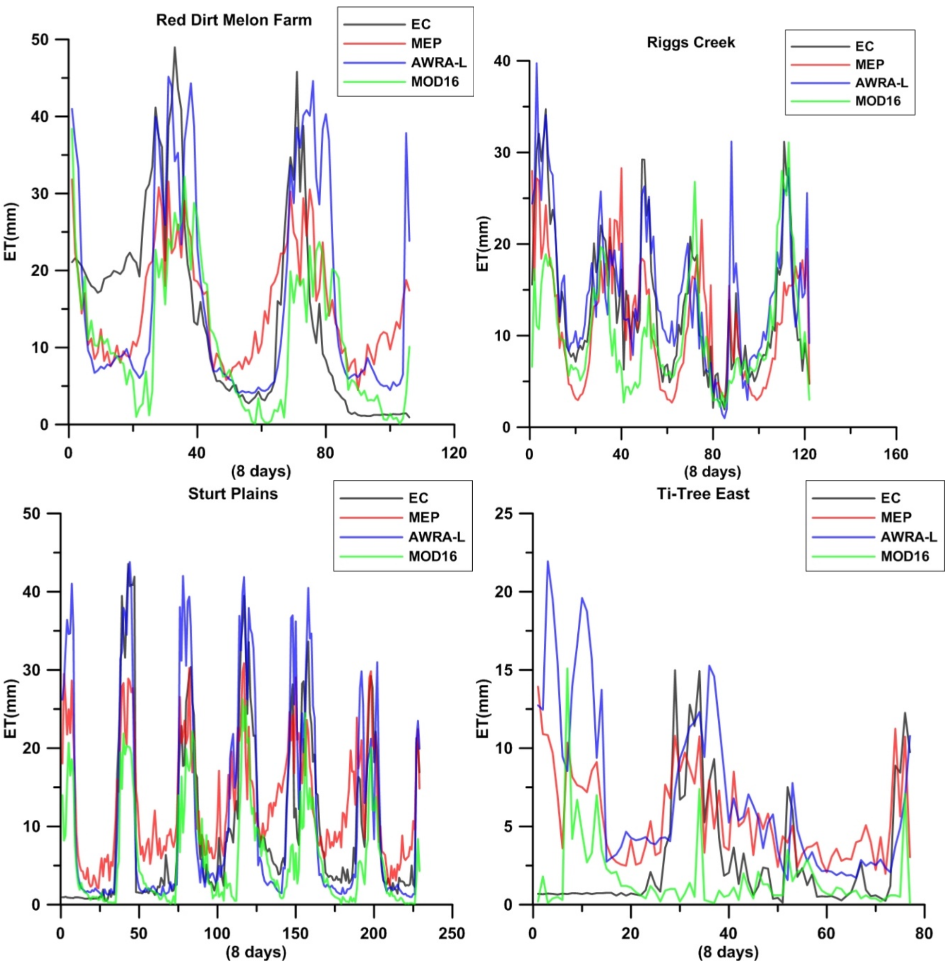

https://doi.org/10.5194/essd-2019-70
Preprint. Discussion started: 18 July 2019




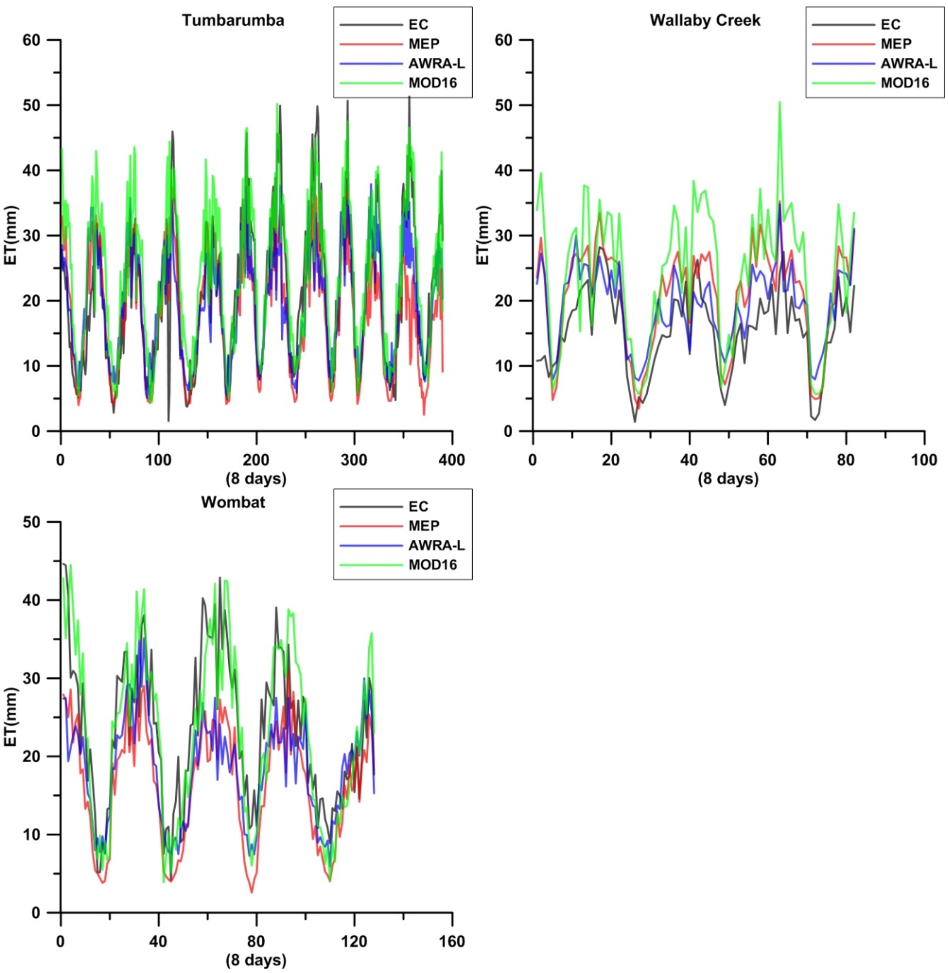


*Figure 4: Continuous plot of the MEP, EC, AWRA-L and MOD16 ET*

Fig. 4 shows that the MEP model reasonably captures the temporal trends of ET relative to the EC flux at most sites. The MEP model appears to underestimate ET in the winter months and overestimate ET in the summer months at the Whroo site. A possible reason for this trend in the MEP model is the wrong classification of the vegetation at the Whroo site. The Whroo site, a box woodland revegetation from the gold mining era currently covered with pasture and eucalyptus species vegetation, is incorrectly classified by the IGBP as an evergreen broadleaved forest. The FPAR product used in partitioning net radiation between soil and canopy show large inter-annual variation, leading to seasonal under- or overestimation of ET.

https://doi.org/10.5194/essd-2019-70
Preprint. Discussion started: 18 July 2019


The MOD16 performs the best at forested sites showing consistent temporal patterns relative to the EC observations. The calibrated AWRA-L model also effectively replicates the temporal trends across most sites and outperforms the MOD16 at most sites.

The accuracy of the modelled ET is strongly affected by the estimated soil water potential using the pedotransfer function. The difference in the footprints of the flux towers may also contribute to the underestimation of ET particularly at flux tower sites with mixed vegetation.

### 3.3 Comparison of the MEP, MOD16 and AWRA-L at Continental scale

A continental scale comparison of the MEP, MOD16 and AWRA_L ET products was carried out after calculating a mean annual ET over the study period from each product over the entire Australia. All 260,000 pixels of 5 km resolution across the three models are used in the analysis. Annual mean ET over Australia from the MEP, MOD16 and AWRA_L products over the 11-year study period were calculated as 440, 262 and 428 mm, respectively. All the corresponding cells were also used to calculate the correlation R, RMSE, NSE and MAE (Table 3). The spatial agreements across the products was evident with all three products showing higher ET around the coastline and lower ET in inland Australia. The NSE between the MEP and AWRA-L shows a better agreement than between the MEP and MOD16 products, which have a negative NSE. The MAE and RMSE were also significantly lower between the MEP and AWRA-L. The total ET from the MEP and AWRA-L appears more reasonable relative to the annual rainfall over Australia (Fig 2). The annual MEP ET as a percentage of rainfall (Fig 2) is consistent with other studies that about 90% of annual rainfall in Australia is returned to the atmosphere through ET (Chiew et al., 2002;Prosser, 2011). Moreover, significant underestimation of ET by the MOD16 model was observed across the flux tower sites.

Spatial analysis of the three products were also carried out using the percentage difference for MEP vs MOD16, MEP vs AWRA-L and AWRA-L vs MOD16 (Fig 4). MEP ET was significantly higher than MOD16 ET for large swaths of inland Australia while MOD16 was higher around the coastlines, particularly the eastern coastlines and Tasmania. The underestimation of the MOD16 ET at the EC flux tower sites (section 3.3 showing that MOD16 underestimating ET at 17 of the 20 flux sites and by more than 30% in 12 of the sites) is confirmed as shown in Fig. 4(a) and (c). The MOD16 performed better at the evergreen broadleaved forest tower sites close to the coastline where it has better agreement with the MEP. However due to mixed performance of the MEP and

MOD16 model at the flux towers around the south-eastern coastline, it is difficult to draw a definite conclusion on which model performs better. The percentage difference between the MEP and AWRA-L model has a narrower range over large areas of Australia with both models within 50% for Australia. There are two large areas in the south-central to Western Australia where the AWRA-L model significantly underestimates ET. The AWRA-L ET is in the range of 1 – 10 mm/yr over large portion of Western Australia with numerous pixels having mean ET less than 1 mm/yr between 2003 and 2013, which may be due to water balance errors in the AWRA-L algorithm. The historic average precipitation in the partially vegetated region is in the range 200-500 mm/yr and it appears implausible for ET to be less than 10 mm/yr. The large swath is also conspicuous in the AWRA-L and MOD16 percentage difference map (Fig 4c). The MOD16 model also produces higher ET than the MEP and AWRA-L specifically in regions classified as evergreen broadleaved forests along the coastlines. The overestimation of MOD16 at evergreen broadleaved forests has been documented in literature (Ruhoff et al., 2013;Hu et al., 2015).

*Table 2: The correlation coefficient (R), Root Mean Square Error (RMSE), Nash-Sutcliffe Efficiency (NSE) and Mean Absolute Error (MAE) for comparison of the MEP, MOD16 and AWRA_L products over the entire Australia*

| RMSE (mm/yr) | | | | | MAE (mm/yr) | | | | |
|---|---|---|---|---|---|---|---|---|---|
| | | MEP | MOD16 | AWRA-L | | | MEP | MOD16 | AWRA-L |
| R | MEP | | 242 | 162 | NSE | MEP | | 203 | 126 |
| | MOD16 | 0.75 | | 205 | | MOD16 | -0.05 | | 187 |
| | AWRA-L | 0.77 | 0.86 | | | AWRA-L | 0.51 | 0.25 | |

https://doi.org/10.5194/essd-2019-70
Preprint. Discussion started: 18 July 2019


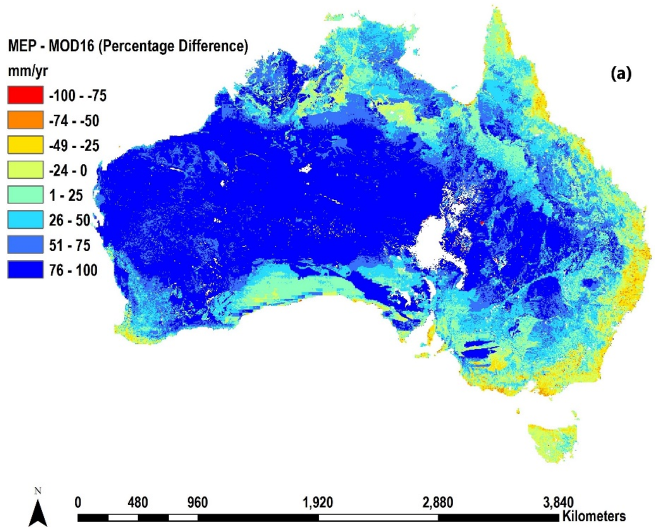


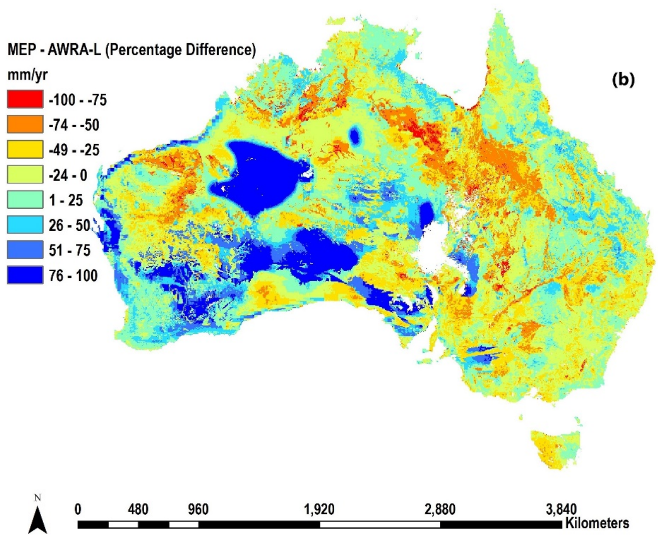

https://doi.org/10.5194/essd-2019-70
Preprint. Discussion started: 18 July 2019


Open Access Earth System Science Data Discussions

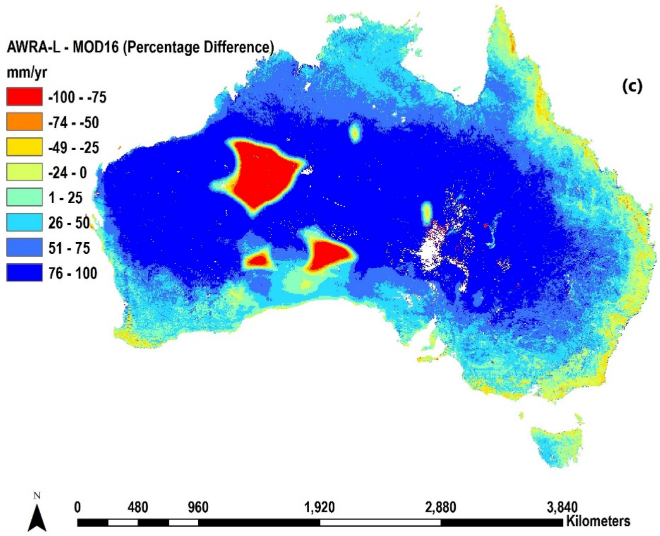


*Figure 5: Mean annual percentage difference between (a) MEP – MOD16; (b) MEP-AWRA-L; (c) AWRA-L-*

### 3.4 Possible challenges with the MEP model

The MEP model appears lacking spatial continuity, probably due to the use of pedotransfer functions to determine the wilting point and field capacity, since surface specific humidity is a crucial input of the MEP model. Hence, further improvement to the MEP model may be achieved by improving the parameterization of the pedotransfer functions for each soil type.

Another challenge is the spatial resolution of soil moisture data for the regions where soil moisture is spatially more variable. The low correlation of the MEP model in the Fogg Dam wetlands may be related to high spatial variability of the soil moisture with intermittent flooding occurring at the site.

https://doi.org/10.5194/essd-2019-70
Preprint. Discussion started: 18 July 2019

Open Access Earth System Science Data Discussions

## 4 Data Availability

The produced daily evaporation and transpiration datasets over the entire Australia at the 5 km resolution for the time period 2003 – 2013 (Abiodun et al., 2019) are publicly available at http://dx.doi.org/10.25901/5ce795d313db8 or from the direct download portal; https://dap.tern.org.au/thredds/catalog/MEP/catalog.html

## 5 Conclusion

We have implemented the MEP model for estimating ET on a continental scale using readily available remote sensing datasets to produce daily evaporation and transpiration at 5 $km^2$ resolution dataset over the entire Australia.

The MEP modelled ET was validated at 20 EC flux tower sites and compared to the MOD16 and AWRA-L model ET. The MEP model outperforms both models at most EC flux sites with the AWRA-L model performing the next best. The MEP ET has the best average RMSE, MAE, R and PBIAS across all 20 EC flux sites. The MEP annual mean ET over Australia corroborates previous studies on the ET trend over Australia indicated by close correlation between MEP ET and rainfall during and after the "millennium drought" period.

The MEP model is the simplest of the three models in terms of model formula and input data. This study shows that the MEP model as a two-source surface energy balance model effectively estimates ET on regional scales using fewer input data to produce evaporation and transpiration separately.

The MEP method has the potential to be further improved for modelling ET. Further study will seek to improve the resolution of the MEP ET product while focusing on the development of a daily global MEP product.

## Appendix A

The MEP model of evaporation and transpiration was derived from the dissipation function in Equation (A1) in (Wang and Bras (2011)

$$D(E, G, H) \equiv \frac{2E^2}{I_e} + \frac{2G^2}{I_s} + \frac{2H^2}{I_a} \quad \text{(A1)}$$

where $I_e, I_s,$ and $I_a$ are the thermal inertia relative to latent heat, ground heat and sensible heat flux, respectively,

$$I_s = \left(2.1\rho^{\left[1.2-0.02\left(\frac{\rho}{\rho_w}\right)100\theta\right]} e^{\left[-0.007\left(\frac{100\theta\rho}{\rho_w}-20\right)^2\right]} + \rho^{\left[0.8+0.02\left(\frac{\rho}{\rho_w}\right)100\theta\right]}\right)^{0.5} \times \left(\frac{\left(\frac{20\theta}{\rho_w}\right)\rho^2}{0.01}\right) \quad \text{(A2)}$$

$I_s$ is parameterized as a function of soil moisture and water density and bulk density (Ma and Xue, 1990;Cai et al., 2007) where $\rho_w$ is density of water ($kg/m^3$); $\theta$ is the soil moisture content of the soil ($m^3/m^3$);

https://doi.org/10.5194/essd-2019-70
Preprint. Discussion started: 18 July 2019


$$I_o = C_o \rho_a C_p \sqrt{kz}\left(\frac{kgz}{\rho_a C_p T_r}\right)^{\frac{1}{6}} \quad \text{(A3)}$$

$C_o$ is the empirical constant characterizing the atmospheric stability (Businger et al., 1971): $C_o = 1.7$ Unstable, 1.2 Stable; $\rho_a$ is the density of air (Kgm$^{-3}$); $k$ = 0.4 the von Kármán constant; $z$ is the distance above the target surface for which the Monin-Obukhov similarity theory is valid (m); $g$ = 9.8 m/s$^2$ the acceleration due to gravity; $T_r$ (~ 300 K) is an atmospheric reference temperature;

$$I_a = I_o|H|^{-\frac{1}{6}},\ I_e = \sigma I_a, \quad \text{(A4)}$$

where $\sigma$ is defined in Equation 2

In the MEP equation over vegetated land surface in Wang and Bras (2011), the reciprocal Bowen ratio; $\beta(\sigma) = 6\left(\sqrt{1+\frac{11}{36}\sigma} - 1\right)$, was introduced to represent the target surface conditions as a function of specific humidity and temperature. Hence, the MEP flux equations over vegetated land can be written as,

$$E_v = \frac{R_{n\_v}}{1+\beta(\sigma)_v^{-1}},\ H_v = \frac{R_{n\_v}}{1+\beta(\sigma)_v} \quad \text{(A5)}$$

At regional scales where air specific humidity and air temperature are used as surrogates of canopy surface specific humidity and temperature, $\beta(\sigma)$ in equation A5 is replaced with $\sigma$

$$\theta\ @FC = 7.561 + 1.176Clay - 0.009843Clay^2 + 0.2132Silt \quad \text{(A6)}$$

$$\theta\ @PWP = -1.304 + 1.117Clay - 0.009309Clay^2 \quad \text{(A7)}$$

Pedotransfer functions in Equations A6 and A7 are used to determine the soil moisture content at field capacity and permanent wilting point as the inputs into the Hutson and Cass model in Equation. FC is the field capacity (-); Clay and Silt are the clay and silt fraction of the soil; and PWP is permanent wilting point (-).

**Acknowledgement**

We would like to acknowledge the invaluable advice of Dr John Hutson in the preparation of this manuscript.

This work used eddy covariance data acquired and shared by the FLUXNET community, including these networks: OzFlux-TERN. The ERA-Interim reanalysis data are provided by ECMWF and processed by LSCE. The FLUXNET eddy covariance data processing and harmonization was carried out by the European Fluxes

Database Cluster, AmeriFlux Management Project, and Fluxdata project of FLUXNET, with the support of CDIAC and ICOS Ecosystem Thematic Center, and the OzFlux, ChinaFlux and AsiaFlux offices.

**References**

Abiodun, O., Batelaan, O., Guan, H., and Wang, J.: A Maximum Entropy Production evaporation and transpiration dataset at 0.05 degree across Australia for 2003 -2013, TERN Geospatial Catalogue, http://dx.doi.org/10.25901/5ce795d313db8, 2019.

Allen, R. G., Tasumi, M., and Trezza, R.: Satellite-based energy balance for mapping evapotranspiration with internalized calibration (METRIC) - Model, Journal of Irrigation and Drainage Engineering, 133, 380-394, 10.1061/(Asce)0733-9437(2007)133:4(380), 2007.

Bastiaanssen, W. G. M., Menenti, M., Feddes, R. A., and Holtslag, A. A. M.: A remote sensing surface energy balance algorithm for land (SEBAL) - 1. Formulation, Journal of Hydrology, 212, 198-212, Doi 10.1016/S0022-1694(98)00253-4, 1998.

Bhattarai, N., Shaw, S. B., Quackenbush, L. J., Im, J., and Niraula, R.: Evaluating five remote sensing based single-source surface energy balance models for estimating daily evapotranspiration in a humid subtropical climate, International Journal of Applied Earth Observation and Geoinformation, 49, 75-86, 10.1016/j.jag.2016.01.010, 2016.

Businger, J. A., Wyngaard, J. C., Izumi, Y., and Bradley, E. F.: Flux-Profile Relationships in Atmospheric Surface Layer, J. Atmos. Sci., 28, 181-&, Doi 10.1175/1520-0469(1971)028<0181:Fprita>2.0.Co;2, 1971.

Cai, G., Xue, Y., Hu, Y., Wang, Y., Guo, J., Luo, Y., Wu, C., Zhong, S., and Qi, S.: Soil moisture retrieval from MODIS data in Northern China Plain using thermal inertia model, International Journal of Remote Sensing, 28, 3567-3581, Doi 10.1080/01431160601034886, 2007.

Chavez, J. L., Gowda, P. H., Howell, T. A., Neale, C. M. U., and Copeland, K. S.: Estimating hourly crop ET using a two-source energy balance model and multispectral airborne imagery, Irrigation Science, 28, 79-91, 10.1007/s00271-009-0177-9, 2009.

Chiew, F., Wang, Q., McConachy, F., James, R., Wright, W., and deHoedt, G.: Evapotranspiration maps for Australia, Water Challenge: Balancing the Risks: Hydrology and Water Resources Symposium 2002, 2002, 167,

Chirouze, J., Boulet, G., Jarlan, L., Fieuzal, R., Rodriguez, J. C., Ezzahar, J., Er-Raki, S., Bigeard, G., Merlin, O., Garatuza-Payan, J., Watts, C., and Chehbouni, G.: Intercomparison of four remote-sensing-based energy balance methods to retrieve surface evapotranspiration and water stress of irrigated fields in semi-arid climate, Hydrol Earth Syst Sc, 18, 1165-1188, 10.5194/hess-18-1165-2014, 2014.

Choi, M., Kustas, W. P., Anderson, M. C., Allen, R. G., Li, F. Q., and Kjaersgaard, J. H.: An intercomparison of three remote sensing-based surface energy balance algorithms over a corn and soybean production region (Iowa, US) during SMACEX, Agricultural and Forest Meteorology, 149, 2082-2097, 10.1016/j.agrformet.2009.07.002, 2009.

Cleugh, H. A., Leuning, R., Mu, Q. Z., and Running, S. W.: Regional evaporation estimates from flux tower and MODIS satellite data, Remote Sensing of Environment, 106, 285-304, 10.1016/j.rse.2006.07.007, 2007.

Colaizzi, P. D., Kustas, W. P., Anderson, M. C., Agam, N., Tolk, J. A., Evett, S. R., Howell, T. A., Gowda, P. H., and O'Shaughnessy, S. A.: Two-source energy balance model estimates of evapotranspiration

https://doi.org/10.5194/essd-2019-70
Preprint. Discussion started: 18 July 2019


using component and composite surface temperatures, Adv Water Resour, 50, 134-151, 10.1016/j.advwatres.2012.06.004, 2012.

Cresswell, H. P., and Paydar, Z.: Water retention in Australian soils. I. Description and prediction using parametric functions, Soil Research, 34, 195-212, 1996.

de Arruda Souza, V., Roberti, D. R., Zimmer, T., Ruhoff, A., Santini Adamatti, D., de Cassia Marques Alves, R., Bortoluzzi Diaz, M., Gonçalves de Gonçalves, L. G., and Leal de Moraes, O. L.: What drives evapotranspiration over irrigated cropland? A comparison between flux tower measurements and MODIS remote sensing estimations, EGU General Assembly Conference Abstracts, 2018, 11010,

Diarra, A., Jarlan, L., Er-Raki, S., Le Page, M., Aouade, G., Tavernier, A., Boulet, G., Ezzahar, J., Merlin, O., and Khabba, S.: Performance of the two-source energy budget (TSEB) model for the monitoring of evapotranspiration over irrigated annual crops in North Africa, Agr Water Manage, 193, 71-88, 10.1016/j.agwat.2017.08.007, 2017.

Dorigo, W., Wagner, W., Albergel, C., Albrecht, F., Balsamo, G., Brocca, L., Chung, D., Ertl, M., Forkel, M., Gruber, A., Haas, E., Hamer, P. D., Hirschi, M., Ikonen, J., de Jeu, R., Kidd, R., Lahoz, W., Liu, Y. Y., Miralles, D., Mistelbauer, T., Nicolai-Shaw, N., Parinussa, R., Pratola, C., Reimer, C., van der Schalie, R., Seneviratne, S. I., Smolander, T., and Lecomte, P.: ESA CCI Soil Moisture for improved Earth system understanding: State-of-the art and future directions, Remote Sensing of Environment, 203, 185-215, 10.1016/j.rse.2017.07.001, 2017.

Gao, Y., and Long, D.: Intercomparison of remote sensing ‐ based models for estimation of evapotranspiration and accuracy assessment based on SWAT, Hydrological processes, 22, 4850-4869, 2008.

Gaur, N., Mohanty, B. P., and Kefauver, S. C.: Effect of observation scale on remote sensing based estimates of evapotranspiration in a semi-arid row cropped orchard environment, Precision Agriculture, 18, 762-778, 10.1007/s11119-016-9486-1, 2017.

Gruber, A., Dorigo, W. A., Crow, W., and Wagner, W.: Triple Collocation-Based Merging of Satellite Soil Moisture Retrievals, Ieee Transactions on Geoscience and Remote Sensing, 55, 6780-6792, 10.1109/Tgrs.2017.2734070, 2017.

Guerschman, J. P., Van Dijk, A. I. J. M., Mattersdorf, G., Beringer, J., Hutley, L. B., Leuning, R., Pipunic, R. C., and Sherman, B. S.: Scaling of potential evapotranspiration with MODIS data reproduces flux observations and catchment water balance observations across Australia, Journal of Hydrology, 369, 107-119, 10.1016/j.jhydrol.2009.02.013, 2009.

Hu, G. C., Jia, L., and Menenti, M.: Comparison of MOD16 and LSA-SAF MSG evapotranspiration products over Europe for 2011, Remote Sensing of Environment, 156, 510-526, 10.1016/j.rse.2014.10.017, 2015.

Huang, S. Y., Deng, Y., and Wang, J. F.: Revisiting the global surface energy budgets with maximum-entropy-production model of surface heat fluxes, Climate Dynamics, 49, 1531-1545, 10.1007/s00382-016-3395-x, 2017.

Hutson, J., and Cass, A.: A retentivity function for use in soil–water simulation models, Journal of Soil Science, 38, 105-113, 1987.

Jeffrey, S. J., Carter, J. O., Moodie, K. B., and Beswick, A. R.: Using spatial interpolation to construct a comprehensive archive of Australian climate data, Environmental Modelling & Software, 16, 309-330, http://dx.doi.org/10.1016/S1364-8152(01)00008-1, 2001.

Jia, Z. Z., Liu, S. M., Xu, Z. W., Chen, Y. J., and Zhu, M. J.: Validation of remotely sensed evapotranspiration over the Hai River Basin, China, J Geophys Res-Atmos, 117, D13113, 10.1029/2011jd017037, 2012.

Johnston, R. M., Barry, S. J., Bleys, E., Bui, E. N., Moran, C. J., Simon, D. A. P., Carlile, P., McKenzie, N. J., Henderson, B. L., Chapman, G., Imhoff, M., Maschmedt, D., Howe, D., Grose, C., Schoknecht, N., Powell, B., and Grundyj, M.: ASRIS: the database, Aust J Soil Res, 41, 1021-1036, 10.1071/Sr02033, 2003.

Jung, M., Reichstein, M., Ciais, P., Seneviratne, S. I., Sheffield, J., Goulden, M. L., Bonan, G., Cescatti, A., Chen, J. Q., de Jeu, R., Dolman, A. J., Eugster, W., Gerten, D., Gianelle, D., Gobron, N., Heinke, J.,

https://doi.org/10.5194/essd-2019-70
Preprint. Discussion started: 18 July 2019


Kimball, J., Law, B. E., Montagnani, L., Mu, Q. Z., Mueller, B., Oleson, K., Papale, D., Richardson, A. D., Roupsard, O., Running, S., Tomelleri, E., Viovy, N., Weber, U., Williams, C., Wood, E., Zaehle, S., and Zhang, K.: Recent decline in the global land evapotranspiration trend due to limited moisture supply, Nature, 467, 951-954, 10.1038/nature09396, 2010.

Kalma, J. D., McVicar, T. R., and McCabe, M. F.: Estimating land surface evaporation: A review of methods using remotely sensed surface temperature data, Surveys in Geophysics, 29, 421-469, 2008.

Khan, M. S., Liaqat, U. W., Baik, J., and Choi, M.: Stand-alone uncertainty characterization of GLEAM, GLDAS and MOD16 evapotranspiration products using an extended triple collocation approach, Agricultural and Forest Meteorology, 252, 256-268, 10.1016/j.agrformet.2018.01.022, 2018.

Kim, H. W., Hwang, K., Mu, Q., Lee, S. O., and Choi, M.: Validation of MODIS 16 global terrestrial evapotranspiration products in various climates and land cover types in Asia, KSCE Journal of Civil Engineering, 16, 229-238, 2012.

Kustas, W. P., and Norman, J. M.: Evaluation of soil and vegetation heat flux predictions using a simple two-source model with radiometric temperatures for partial canopy cover, Agricultural and Forest Meteorology, 94, 13-29, Doi 10.1016/S0168-1923(99)00005-2, 1999.

Liaqat, U. W., and Choi, M.: Accuracy comparison of remotely sensed evapotranspiration products and their associated water stress footprints under different land cover types in Korean peninsula, Journal of Cleaner Production, 155, 93-104, 10.1016/j.jclepro.2016.09.022, 2017.

Liu, Y. Y., Dorigo, W. A., Parinussa, R. M., de Jeu, R. A. M., Wagner, W., McCabe, M. F., Evans, J. P., and van Dijk, A. I. J. M.: Trend-preserving blending of passive and active microwave soil moisture retrievals, Remote Sensing of Environment, 123, 280-297, 10.1016/j.rse.2012.03.014, 2012.

Long, D., Longuevergne, L., and Scanlon, B. R.: Uncertainty in evapotranspiration from land surface modeling, remote sensing, and GRACE satellites, Water Resources Research, 50, 1131-1151, 2014.

Ma, A., and Xue, Y.: A study of remote sensing information model of soil moisture, Proceedings of the 11th Asian conference on remote sensing, 1990, pp ‐ 11,

Mark, F., and Damien, S.-M.: MCD12C1 MODIS/Terra+Aqua Land Cover Type Yearly L3 Global 0.05Deg CMG V006 [Data set], NASA EOSDIS Land Processes DAAC, 10.5067/MODIS/MCD12C1.006, 2015.

Minasny, B., McBratney, A. B., and Bristow, K. L.: Comparison of different approaches to the development of pedotransfer functions for water-retention curves, Geoderma, 93, 225-253, Doi 10.1016/S0016-7061(99)00061-0, 1999.

Minasny, B., and Mcbratney, A. B.: The neuro-m method for fitting neural network parametric pedotransfer functions Soil Sci Soc Am J, 66, 1407-1407, 2002.

Mu, Q., Heinsch, F. A., Zhao, M., and Running, S. W.: Development of a global evapotranspiration algorithm based on MODIS and global meteorology data, Remote Sensing of Environment, 111, 519-536, DOI 10.1016/j.rse.2007.04.015, 2007.

Mu, Q. Z., Zhao, M. S., and Running, S. W.: Improvements to a MODIS global terrestrial evapotranspiration algorithm, Remote Sensing of Environment, 115, 1781-1800, 10.1016/j.rse.2011.02.019, 2011.

Myneni, R., Knyazikhin, Y., and Park, T.: MOD15A2H MODIS/terra leaf area index/FPAR 8-day L4 global 500 m SIN grid V006, NASA EOSDIS Land Processes DAAC, http://doi.org/10.5067/MODIS/MOD15A2H.006, 2015.

Najmaddin, P. M., Whelan, M. J., and Balzter, H.: Estimating Daily Reference Evapotranspiration in a Semi-Arid Region Using Remote Sensing Data, Remote Sensing, 9, 779, ARTN 779

10.3390/rs9080779, 2017.

Nearing, G. S., Moran, M. S., Scott, R. L., and Ponce-Campos, G.: Coupling diffusion and maximum entropy models to estimate thermal inertia, Remote Sensing of Environment, 119, 222-231, 10.1016/j.rse.2011.12.012, 2012.

Norman, J., Kustas, W., Prueger, J., and Diak, G.: Surface flux estimation using radiometric temperature: A dual ‐ temperature ‐ difference method to minimize measurement errors, Water Resources Research, 36, 2263-2274, 2000.

https://doi.org/10.5194/essd-2019-70
Preprint. Discussion started: 18 July 2019


Norman, J. M., Anderson, M. C., Kustas, W. P., French, A. N., Mecikalski, J., Torn, R., Diak, G. R., Schmugge, T. J., and Tanner, B. C. W.: Remote sensing of surface energy fluxes at 10(1)-m pixel resolutions, Water Resources Research, 39, 18, Artn 1221

10.1029/2002wr001775, 2003.

Prosser, I. P.: Water: science and solutions for Australia, CSIRO, 2011.

Rab, M. A., Chandra, S., Fisher, P. D., Robinson, N. J., Kitching, M., Aumann, C. D., and Imhof, M.: Modelling and prediction of soil water contents at field capacity and permanent wilting point of dryland cropping soils, Soil Research, 49, 389-407, 10.1071/Sr10160, 2011.

Roerink, G. J., Su, Z., and Menenti, M.: S-SEBI: A simple remote sensing algorithm to estimate the surface energy balance, Phys. Chem. Earth Pt B-Hydrol. Oceans Atmos., 25, 147-157, Doi 10.1016/S1464-1909(99)00128-8, 2000.

Ruhoff, A. L., Paz, A. R., Aragao, L. E. O. C., Mu, Q., Malhi, Y., Collischonn, W., Rocha, H. R., and Running, S. W.: Assessment of the MODIS global evapotranspiration algorithm using eddy covariance measurements and hydrological modelling in the Rio Grande basin, Hydrolog Sci J, 58, 1658-1676, 10.1080/02626667.2013.837578, 2013.

Senay, G. B., Bohms, S., Singh, R. K., Gowda, P. H., Velpuri, N. M., Alemu, H., and Verdin, J. P.: Operational Evapotranspiration Mapping Using Remote Sensing and Weather Datasets: A New Parameterization for the SSEB Approach, J Am Water Resour As, 49, 577-591, 10.1111/jawr.12057, 2013.

Shanafield, M., Cook, P. G., Gutierrez-Jurado, H. A., Faux, R., Cleverly, J., and Eamus, D.: Field comparison of methods for estimating groundwater discharge by evaporation and evapotranspiration in an arid-zone playa, Journal of Hydrology, 527, 1073-1083, 10.1016/j.jhydrol.2015.06.003, 2015.

Song, L. S., Liu, S. M., Kustas, W. P., Zhou, J., Xu, Z. W., Xia, T., and Li, M. S.: Application of remote sensing-based two-source energy balance model for mapping field surface fluxes with composite and component surface temperatures, Agricultural and Forest Meteorology, 230, 8-19, 10.1016/j.agrformet.2016.01.005, 2016.

Sun, Z. G., Wang, Q. X., Matsushita, B., Fukushima, T., Ouyang, Z., and Watanabe, M.: Development of a Simple Remote Sensing EvapoTranspiration model (Sim-ReSET): Algorithm and model test, Journal of Hydrology, 376, 476-485, 10.1016/j.jhydrol.2009.07.054, 2009.

Tang, Q., Peterson, S., Cuenca, R. H., Hagimoto, Y., and Lettenmaier, D. P.: Satellite‐based near‐real‐time estimation of irrigated crop water consumption, Journal of Geophysical Research: Atmospheres, 114, 2009.

Tang, R. L., Shao, K., Li, Z. L., Wu, H., Tang, B. H., Zhou, G. Q., and Zhang, L.: Multiscale Validation of the 8-day MOD16 Evapotranspiration Product Using Flux Data Collected in China, Ieee J-Stars, 8, 1478-1486, 10.1109/Jstars.2015.2420105, 2015.

Timmermans, W. J., Kustas, W. P., Anderson, M. C., and French, A. N.: An intercomparison of the surface energy balance algorithm for land (SEBAL) and the two-source energy balance (TSEB) modeling schemes, Remote Sensing of Environment, 108, 369-384, 2007.

Velpuri, N. M., Senay, G. B., Singh, R. K., Bohms, S., and Verdin, J. P.: A comprehensive evaluation of two MODIS evapotranspiration products over the conterminous United States: Using point and gridded FLUXNET and water balance ET, Remote Sensing of Environment, 139, 35-49, 2013.

Wan, Z. M., Zhang, Y. L., Zhang, Q. C., and Li, Z. L.: Validation of the land-surface temperature products retrieved from Terra Moderate Resolution Imaging Spectroradiometer data, Remote Sensing of Environment, 83, 163-180, Doi 10.1016/S0034-4257(02)00093-7, 2002.

Wan, Z. M.: New refinements and validation of the collection-6 MODIS land-surface temperature/emissivity product, Remote Sensing of Environment, 140, 36-45, 10.1016/j.rse.2013.08.027, 2014.

Wang, J. F., and Bras, R. L.: A model of evapotranspiration based on the theory of maximum entropy production, Water Resources Research, 47, Artn W03521

10.1029/2010wr009392, 2011.

https://doi.org/10.5194/essd-2019-70
Preprint. Discussion started: 18 July 2019


Wang, Y. Q., Xiong, Y. J., Qiu, G. Y., and Zhang, Q. T.: Is scale really a challenge in evapotranspiration estimation? A multi-scale study in the Heihe oasis using thermal remote sensing and the three-temperature model, Agricultural and Forest Meteorology, 230-231, 128-141, 10.1016/j.agrformet.2016.03.012, 2016.

Williams, J., Ross, P., and Bristow, K.: Prediction of the Campbell water retention function from texture, structure, and organic matter. p. 427–442. M. Th. van Genuchten et al.(ed.) Proc. Int. Worksh. on Indirect Methods for Estimating the Hydraulic Properties of Unsaturated Soils, Riverside, CA. 11–13 Oct. 1989. US Salinity Lab., Riverside, CA, 1992, -,

Xiong, Y. J., Qiu, G. Y., Zhao, S. H., and Tian, F.: Estimating regional evapotranspiration using a three-temperature model and MODIS products, Remote Sensing of the Terrestrial Water Cycle, 206, 83, 2014.

Yang, J. C., and Wang, Z. H.: Land surface energy partitioning revisited: A novel approach based on single depth soil measurement, Geophysical Research Letters, 41, 8348-8358, 10.1002/2014gl062041, 2014.

Yang, Y., Long, D., Guan, H., Liang, W., Simmons, C., and Batelaan, O.: Comparison of three dual‐source remote sensing evapotranspiration models during the MUSOEXE‐12 campaign: Revisit of model physics, Water Resources Research, 51, 3145-3165, 2015.

Yang, Y. M., Qiu, J. X., Zhang, R. H., Huang, S. F., Chen, S., Wang, H., Luo, J. S., and Fan, Y.: Intercomparison of Three Two-Source Energy Balance Models for Partitioning Evaporation and Transpiration in Semiarid Climates, Remote Sensing, 10, 1149, ARTN 1149, 10.3390/rs10071149, 2018.

Zhang, K., Kimball, J. S., and Running, S. W.: A review of remote sensing based actual evapotranspiration estimation, Wiley Interdisciplinary Reviews: Water, 3, 834-853, 2016.

Zhang, R., Sun, X., Wang, W. M., P. Xu, J., Zhu, Z., and Tian, J.: An operational two-layer remote sensing model to estimate surface flux in regional scale: Physical background, 225-244 pp., 2005.